Chem

Article

Light-driven ratcheted formation of diastereomeric host-guest systems

Graphical abstract

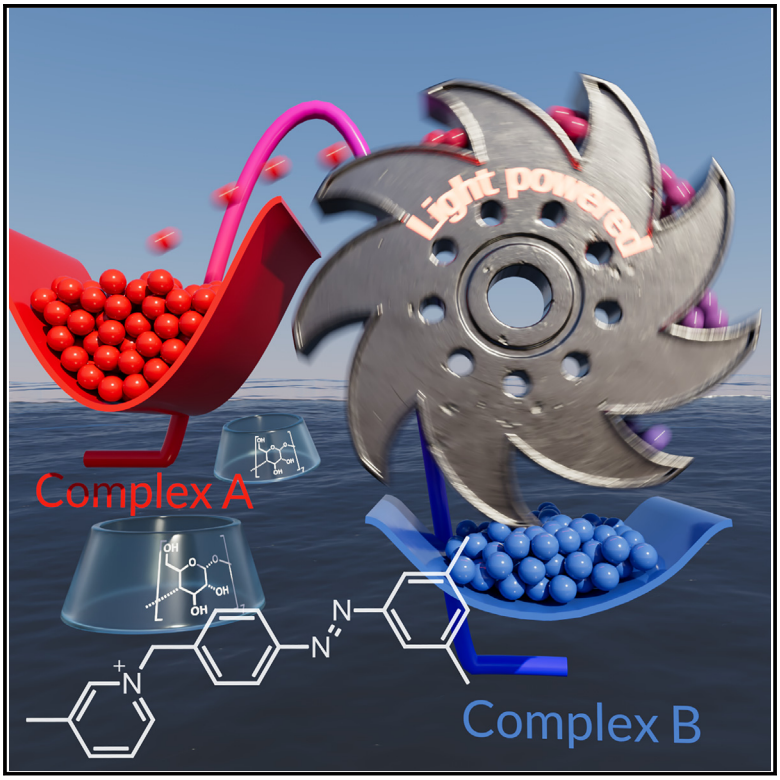

Highlights

- Diastereomeric complexes between azobenzene derivatives and cyclodextrin
- Selective formation of high-energy diastereomers driven by visible light
- Photochemical reaction network with non-equilibrium product distribution
- Light-ratcheted self-assembly amenable to biologically relevant applications

Authors

Iago Neira, Chiara Taticchi, Federico Nicoli, ..., Serena Silvi, Massimo Baroncini, Alberto Credi

Correspondence

alberto.credi@unibo.it

In brief

The formation of supramolecular complexes is typically a spontaneous equilibrium process that produces the most stable structures. Here, we demonstrate that visible light can be used to favor the formation of less stable, high-energy complexes composed of cyclodextrin and azobenzene derivatives. This represents a rare example of controlled formation of desired structures under non-equilibrium conditions. The operation through visible-light irradiation in water endows this system with remarkable potential for applications in biological environments.

Neira et al., 2025, Chem *11*, 102375
May 8, 2025
https://doi.org/10.1016/j.chempr.2024.11.013

CellPress

Please cite this article in press as: Neira et al., Light-driven ratcheted formation of diastereomeric host-guest systems, Chem (2024), https://doi.org/10.1016/j.chempr.2024.11.013

Chem

CellPress
OPEN ACCESS

Article

Light-driven ratcheted formation of diastereomeric host-guest systems

Iago Neira,[1,2,6] Chiara Taticchi,[2,3,6] Federico Nicoli,[2,3,6] Massimiliano Curcio,[2,3] Marcos D. Garcia,[1] Carlos Peinador,[1] Serena Silvi,[2,4] Massimo Baroncini,[2,5] and Alberto Credi[2,3,7,*]

[1]Centro Interdisciplinar de Química e Bioloxía (CICA) and Departamento de Química, Facultad de Ciencias, Universidade da Coruña, A Coruña, Spain
[2]Center for Light Activated Nanostructures, Istituto ISOF-CNR, Bologna, Italy
[3]Dipartimento di Chimica Industriale "Toso Montanari," Alma Mater Studiorum – Università di Bologna, Bologna, Italy
[4]Dipartimento di Chimica "Giacomo Ciamician," Alma Mater Studiorum – Università di Bologna, Bologna, Italy
[5]Dipartimento di Scienze e Tecnologie Agro-Alimentari, Alma Mater Studiorum – Università di Bologna, Bologna, Italy
[6]These authors contributed equally
[7]Lead contact
*Correspondence: alberto.credi@unibo.it
https://doi.org/10.1016/j.chempr.2024.11.013

THE BIGGER PICTURE Nature performs endergonic reactions by coupling them with exergonic ones. This mechanism underlies the uptake and flow of energy in biochemical networks, enabling its use to achieve specific structures and functions crucial for living systems. Herein, we show how light can drive the self-assembly of artificial molecular components toward a high-energy host-guest complex not afforded under equilibrium. This work represents a rare example of the ratcheted self-assembly of complexes between cyclodextrin and azobenzene guests, which were previously investigated only for their equilibrium behavior. This advancement will expand studies on molecular architectures based on cyclodextrins, offering new perspectives for the realization of active materials. Moreover, since the system operates in water and employs visible light, it is relevant for building artificial molecular machines that operate under physiological conditions, thus representing a significant step toward their practical application.

SUMMARY

The ability to exploit an energy source to drive chemical reactions away from thermodynamic equilibrium is an essential feature of life and a grand challenge for the design of fuel-driven dynamic artificial nanosystems. Here, we investigate the effect of light irradiation on the formation of supramolecular complexes composed of azobenzene-type guests and a cyclodextrin (CD) host in water. Whereas previous studies on these complexes have focused on equilibrium properties, our work explores far-from-equilibrium distributions obtained by light-driven association. We demonstrate that the relative abundance of the two CD orientational diastereomeric complexes can be inverted upon photoirradiation and showcase a ratcheted approach, employing biocompatible macrocycles and harnessing visible light, to the spontaneous formation of high-energy CD complexes with broad applicability in aqueous environments. We foresee opportunities for the development of active materials, the design of artificial metabolic networks, and the engineering of molecular machines operating under physiological conditions.

INTRODUCTION

Cyclodextrins (CDs) are a class of water-soluble macrocycles composed of *n*-glucose units (*n* = 6 in α-CD, *n* = 7 in β-CD, and *n* = 8 in γ-CD)[1] and are capable of forming host-guest complexes with aliphatic and aromatic guests in water.[2,3] These macrocycles lack any plane of symmetry and consist of a wide and a narrow rim; therefore, their combination with non-symmetric (oriented) linear guests leads to the formation of two diastereomeric complexes depending on the relative orientation of the molecular components, i.e., orientational isomers (Figure 1A).[4,5] When the orientational isomers display both different thermodynamic stability and rates of formation, a scenario involving multiple assembling pathways arises.[6–8] A case in point is when the less stable product forms more rapidly, referred to as the transient product (complex A, Figure 1). In line with the Curtin-Hammett principle,[9–14] the energy difference between the threading activation barriers ($\Delta\Delta G^{\ddagger}$) is responsible for the

Please cite this article in press as: Neira et al., Light-driven ratcheted formation of diastereomeric host-guest systems, Chem (2024), https://doi.org/10.1016/j.chempr.2024.11.013

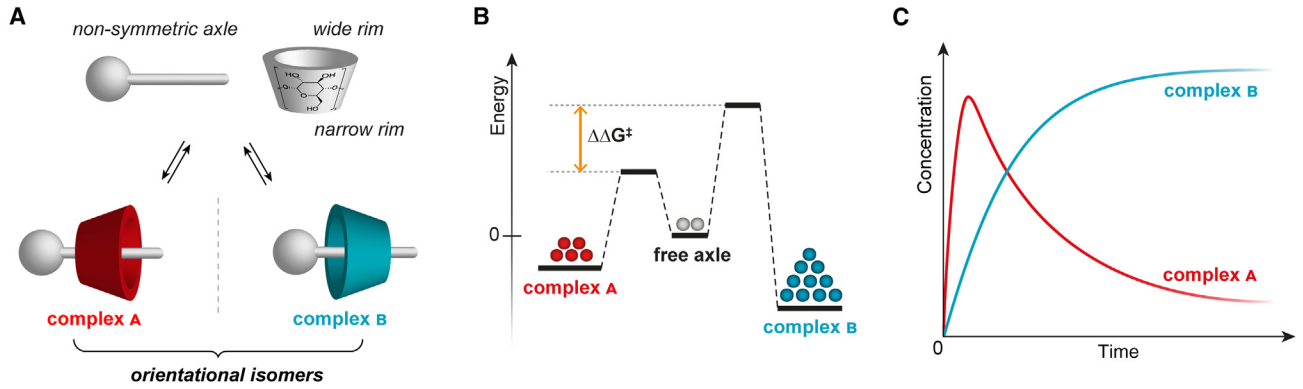

Figure 1. Formation of supramolecular complexes between a cyclodextrin host and non-symmetric axle-type guest

(A) Competitive equilibria between a non-symmetric axle and CD.

(B) Schematic free-energy profiles for the spontaneous host-guest complex formation.

(C) Kinetic profiles showing the transient accumulation of the faster and less stable complex A (kinetic product, red trace) followed by its disassembly, which occurs concomitantly with the formation of complex B (thermodynamic product, blue trace).

transitory accumulation of the kinetic metastable products (Figures 1B and 1C). However, because the host-guest assembly reactions are reversible, the network will evolve toward thermal equilibrium, in which the thermodynamic product prevails (complex B, Figure 1).[14]

The diastereoselective formation of such assemblies can be achieved through the kinetic trapping of the system in local minima.[15–18] However, the direct transformation of the stable isomer (complex B, Figure 1) into the higher-energy one (complex A, Figure 1) is an endergonic process ($\Delta G > 0$),[19] so the consumption of an energy source is required for sustaining a stationary state in which the kinetic product dominates.[20] This approach, recently termed "ratcheting synthesis," involves the consumption of an energy input (fuel) through orthogonal reaction pathways, enabling endergonic processes within a closed network of reactions.[21] In artificial supramolecular systems, ratcheting-assisted assemblies are referred to as "driven self-assemblies," in which the transient products accumulate as a fuel is transformed into a byproduct or byproducts termed "waste."[22,23]

From this perspective, the study of the well-known interaction between CDs and azobenzene derivatives has acquired renewed interest. These inclusion complexes have been thoroughly investigated for the efficient light-induced switching of their association constants at thermodynamic equilibrium,[24] giving rise to applications across diverse fields, e.g., polymeric-responsive materials,[25] phase-transfer systems,[26] cargo-delivery materials,[27,28] supramolecular hydrogels,[29,30] artificial nanochannels,[31] functional surfaces,[32] and the development of artificial molecular machines (AMMs).[24,33,34]

However, the possibility of dynamically accessing non-equilibrium distributions by light irradiation[35–43] has been minimally explored in CD chemistry. In fact, by taking advantage of a ratcheting synthesis approach, it might be possible to operate kinetic control of CD/azobenzene systems to result in a light-driven spontaneous formation. Moreover, considering that diastereomeric orientational isomers can be obtained upon complexation with CDs, such a strategy could be employed to sustain a non-equilibrium diastereomeric excess (de).[44,45]

In this study, we thoroughly investigate the thermodynamics and kinetics of the diastereomeric complexes formed between α-CD and a set of non-symmetric axles incorporating azobenzene units. Our goal is to understand design principles and identify the relevant parameters to shift the focus of these systems from classical thermodynamic host-guest assembly to light-sustained distributions away from thermal equilibrium.

RESULTS

Synthesis and characterization of axles 1–3

Non-symmetric cationic axles 1–3 consist of an azobenzene scaffold endowed with a 3,5-dimethyl stopper unit[6,7,46] and a pyridinium moiety that provides water solubility (Figure 2A). This design allows for the unidirectional complexation with α-CD from the sole pyridinium gate. We chose the pyridinium substituents to yield different threading kinetic parameters by increasing steric hindrance (*t*-Bu >> Me > H). We synthesized the axles according to a divergent synthetic approach: we employed the Mills coupling reaction[47] to prepare the common azobenzene benzyl bromide, which we then functionalized with the corresponding substituted pyridines to yield the target bromide salts. Detailed methods can be found in the supplemental information.

Axles *E*-**1**-*E*-**3** show the typical spectral features of *E*-azobenzene. Upon irradiation at 365 nm, $E \rightarrow Z$ photoisomerization takes place and leads to a photostationary state (PSS) rich in *Z* isomer (>90%). $Z \rightarrow E$ isomerization can be induced both thermally ($t_{1/2}$ > 1 month at room temperature) and photochemically by irradiation with visible light (436 nm), resulting in a PSS with about 70% of the *E* isomer (Figures S30–S38 and Table S6).

When an excess of α-CD was mixed with axle *E*-**1** in deuterated water, the ^{1}H NMR spectrum showed two distinct sets of signals with a negligible amount of free axle (Figure 2B). At chemical equilibrium, one set dominated over the other in a 94:6 ratio, indicating the coexistence of two host-guest orientational isomers in slow exchange on the NMR timescale.

Please cite this article in press as: Neira et al., Light-driven ratcheted formation of diastereomeric host-guest systems, Chem (2024), https://doi.org/10.1016/j.chempr.2024.11.013

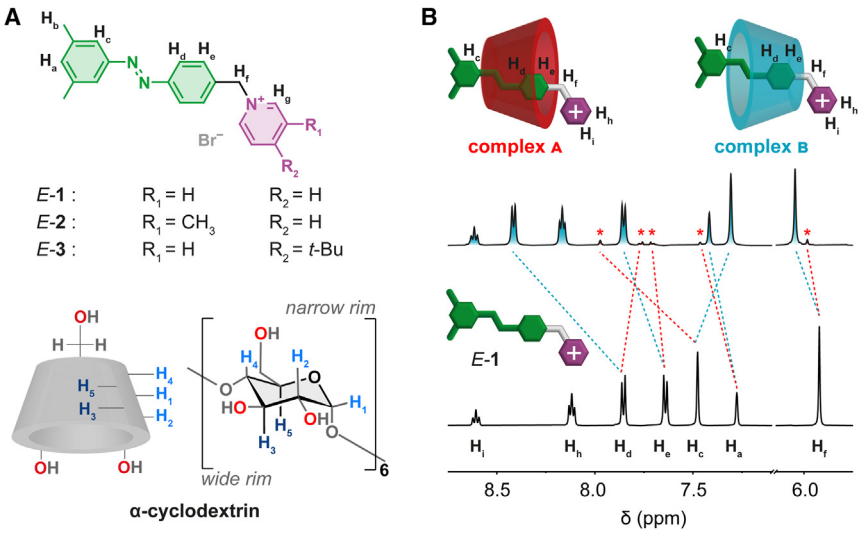

Figure 2. Photoactive axles 1–3 and ^{1}H NMR spectrum of the complex

(A) Molecular structure of axles 1–3 and graphical representation of α-CD and its glycosidic unit; the hydrogen nuclei monitored in ^{1}H NMR experiments are labeled with numbers and letters for the host and guests, respectively.

(B) Stacked partial ^{1}H NMR spectra (500 MHz, D_2O, 298 K). Bottom: free axle *E*-**1**. Top: mixture of complex B (blue peaks) and complex A (red peaks highlighted by asterisks) recorded after equilibrium was reached. Initial concentrations: [*E*-**1**] = 8.0 mM, [α-CD] = 20.0 mM.

In the prevalent species (Figure 2B, blue peaks), the H_c signal underwent an upfield shift ($\Delta\delta = -0.17$ ppm; Figure S14 and Table S1), attributed to the shielding effect provided by the CD hydrophobic cavity. Conversely, the H_d resonance showed significant deshielding ($\Delta\delta = 0.56$ ppm), indicating an interaction with the electronegative primary hydroxyl groups on the α-CD narrow rim.

To further investigate the stereochemical arrangement between the macrocycle and the axle, we performed ^{1}H NMR ROESY experiments.[6,7,45,48] The experiments revealed cross-peaks between the signals of H_c on the axle and H_3 on the CD; moreover, the resonances of H_e correlated with those of H_5 (Figure S17). The combination of 1D and 2D NMR experiments confirmed that in the most abundant product, the wide rim faces the stopper unit, corresponding to complex B (Figure 2B).

In the minor product (Figure 2B, resonances marked by asterisks), the resonance of H_c was deshielded ($\Delta\delta = 0.44$ ppm), suggesting an interaction with the narrow rim. Additionally, a slight shielding effect of the H_d resonance ($\Delta\delta = -0.14$ ppm) points to the inclusion of the photoactive segment into the cavity. These findings indicate that in this complex, the narrow rim faces the stopper unit (Figure 2B, complex A).

Similar results were observed in analogous experiments performed with axles *E*-**2** and *E*-**3** (Figures S15, S16, and S18–S20). Interestingly, the investigation of the self-assembling equilibration through UV-visible (UV-vis) spectroscopy revealed that the A and B isomers exhibited different UV-vis spectra: the π-π* band of both products showed hypochromic and bathochromic effects, which were more pronounced for the A-type and B-type complexes, respectively (Figures S39, S40, and S43). The complexes with axles *E*-**2** and *E*-**3** were also characterized by means of high-resolution mass spectrometry electrospray ionization (HRMS-ESI) (Figures S28 and S29).

Kinetic and thermodynamic analysis

The nature of the substituent on the pyridinium gate directly influences the kinetics of the formation of isomers A and B. At millimolar concentrations and room temperature, the association occurred in minutes for axle *E*-**1**, whereas it required several hours for axles *E*-**2** and *E*-**3**. The faster-equilibrating axle *E*-**1** was examined with equimolar solutions of both the host and the guest. In contrast, axles *E*-**2** and *E*-**3** required higher concentrations and excess of macrocycle because of their slower threading-dethreading kinetics (Figures S21–S23).

Figure 3A shows the complexation kinetics of axle *E*-**2** and α-CD recorded by means of time-resolved ^{1}H NMR spectroscopy. The analysis of the time profile showed that the rapidly forming complex A (red dots) coincides with a metastable kinetic product. The latter is transiently accumulated in the first few minutes before eventually leading to the formation of complex B (blue dots), i.e., the thermodynamic product.

The first instants of the process were monitored by a spectrophotometric stopped-flow technique, which provided higher temporal resolution (Figure 3B). Notably, the kinetic trace recorded for the formation of complex A did not show a marked plateau. This was due to the simultaneous formation of complex B, whose complete threading process was followed via longer recording times by a UV-vis spectrophotometer (Figures 3B [inset] and S47).

At the thermodynamic equilibrium, the distribution of the orientational isomers is composed of 90% of thermodynamic product B and less than 10% of kinetic product A. Similar distributions were observed for the analogous experiment conducted with axle *E*-**1** (Figures S21, S44, and S45), whereby the process occurred in a shorter timescale because substituents were absent from the pyridinium gate. In contrast, axle *E*-**3** exhibited an extremely slow threading profile, ascribed to the presence of the bulky *tert*-butyl group in the *para* position of the pyridinium (Figures S23 and S48). Moreover, the system followed the opposite trend: complex B was formed faster, so the most stable product also had the lower activation barrier. We obtained the kinetic and thermodynamic parameters of axles **1–3** by fitting the experimental traces (Table 1; see additional details in Tables S4, S5, and S7–S9).

The association constants of the B isomers (K_B) were in the order of magnitude 10^4 M^{-1}, consistent with literature reports for similar systems.[29,33] Notably, the association constants of the less stable orientational isomers (K_A) were at least one order of magnitude smaller than those of the corresponding K_B. The higher K_B value is most likely due to the co-conformational

Please cite this article in press as: Neira et al., Light-driven ratcheted formation of diastereomeric host-guest systems, Chem (2024), https://doi.org/10.1016/j.chempr.2024.11.013

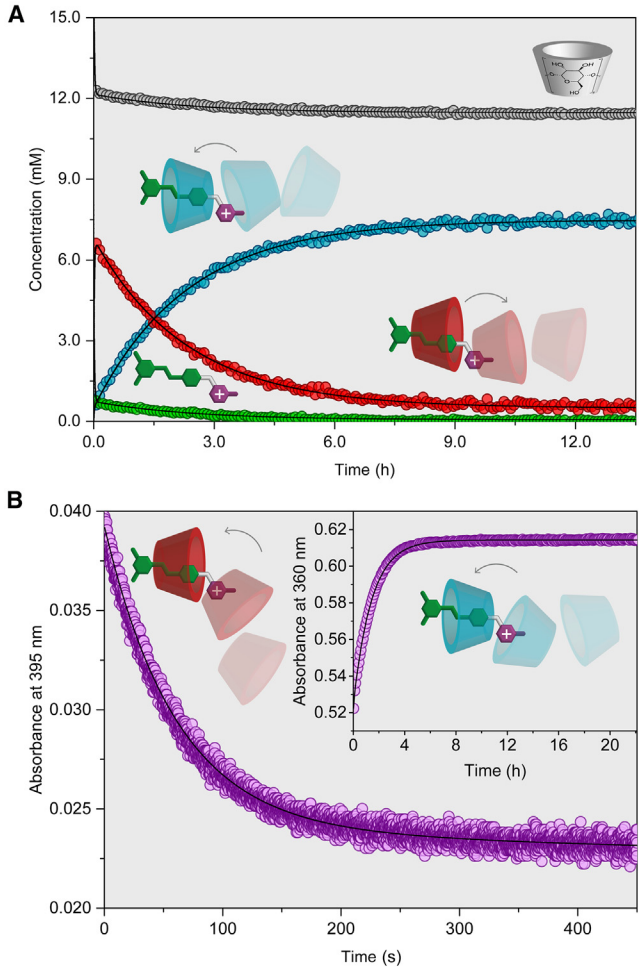

Figure 3. Thermal equilibration of the system composed of *E*-2 and α-CD

(A) ^{1}H NMR concentration profiles (500 MHz, D_2O, 298 K) of the equilibration between axle *E*-**2** (8.0 mM) and α-CD (20.0 mM). In the graph, the concentrations in time of complex A (red dots), complex B (blue dots), free α-CD (gray dots), and free *E*-**2** (green dots) are reported together with the data fit (black lines).

(B) Time-dependent absorption changes at 395 and 360 nm (purple dots) together with the data fit (black line) upon rapid mixing of *E*-**2** and α-CD in H_2O. Final concentrations: [*E*-**2**] = 49.7 μM, [α-CD] = 11.7 mM.

geometry of the B isomers, which favor ion-dipole interactions between the electronegative narrow rim of the CD and the cationic pyridinium gate (Figure 2B).

As a general trend, for both A and B orientational isomers, the kinetic constant values (k_{in} and k_{out}) decreased as the steric hindrance increased. Moreover, the electrostatic interaction between the narrow rim of the host and the cationic gate could have assisted the formation of the fast-forming complex A. This phenomenon justifies the behavior observed in *E*-**1** and *E*-**2**, where the steric hindrance of the gate is less important. In contrast, in *E*-**3**, the bulky *tert*-butyl unit dramatically obstructed threading, and the kinetic rate constant for complex A formation ($k_{A\text{-}in}$) was five orders of magnitude lower than that determined for *E*-**1**.

Table 1. Thermodynamic and kinetic constants for the association process of axles *E*-1–*E*-3 and α-CD

Axle	K_B (10^4 M^{-1})	$k_{B\text{-}in}$ (M^{-1} s^{-1})	K_A (10^4 M^{-1})	$k_{A\text{-}in}$ (M^{-1} s^{-1})	$\Delta\Delta G^\circ$ (kcal mol^{-1})	$\Delta\Delta G^\ddagger$ (kcal mol^{-1})
E-**1**	2.20	22.0	0.13	51.5	1.70	0.50
E-**2**	1.07	9.30×10^{-2}	0.07	1.13	1.60	1.40
E-**3**	1.84	1.64×10^{-3}	0.05	3.40×10^{-4}	2.10	−1.00

K, association constants; k_{in}, kinetic constants of threading; k_{out}, kinetic constants relative to the dethreading of complexes A and B. The difference in free energy for the competitive association was calculated as $\Delta\Delta G^\circ = \Delta G^\circ_A - \Delta G^\circ_B$, where $\Delta G^\circ_A = -RT\ln(K_A)$ and $\Delta G^\circ_B = -RT\ln(K_B)$. The free energy of activation ($\Delta G_{in}^\ddagger$) was calculated with the Eyring equation $\Delta G_{in}^\ddagger = -RT\ln(k_{in}h/k_BT)$, where R, h, and k_B correspond to the gas, Planck, and Boltzmann constants, respectively. The difference in free energy of activation for the competitive association was calculated as $\Delta\Delta G^\ddagger = \Delta G_{B\text{-}in}^\ddagger - \Delta G_{A\text{-}in}^\ddagger$.

The qualitative free-energy profiles for the competitive formation of complexes A and B are reported in Figure 4.

As we compare the values of $\Delta\Delta G^\ddagger$ and the relative energies of the complexes (Figure 4 and Table 1), it becomes evident that the relative stabilities ($\Delta\Delta G^\circ$) of the two orientational isomers are similar for *E*-**1**, *E*-**2**, and *E*-**3**. In contrast, the difference in their activation barriers is more significant. Specifically, both *E*-**1** and *E*-**2** exhibited $\Delta\Delta G^\ddagger > 0$, which means that the insertion of the positively charged pyridinium extremity is kinetically favored through the CD narrow rim with respect to the wider rim. When *E*-**1** was replaced with *E*-**2**, $k_{A\text{-}in}$ decreased by about 50 times, whereas $k_{B\text{-}in}$ dropped by a factor of 240. The effect was reversed for *E*-**3**, whose complex B formed faster than the corresponding A isomer (negative $\Delta\Delta G^\ddagger$).

All together, these observations suggest that the threading kinetics are affected by the interplay of electrostatic and steric effects. For both *E*-**1** and *E*-**2**, the partial negative charge present on the narrow rim might assist the threading of the positively charged end that leads to complex A. The much larger $\Delta\Delta G^\ddagger$ of *E*-**2** than of *E*-**1** (Table 1) indicates that, despite the steric effect added by the methyl group that increases all activation barriers (Table S5), electrostatic interactions still play a predominant role in guiding the association process. On the other hand, if the pyridinium extremity is very bulky, as for *E*-**3**, the steric hindrance dominates, and the insertion through the wider rim becomes the faster route, leading to complex B.

Among the investigated axles, *E*-**2** exhibited the highest $\Delta\Delta G^\ddagger$ value, suggesting that it might provide greater selectivity for the kinetic trapping of the A-type orientational isomer. For this reason, we carried out the following irradiation experiments by exclusively using this axle.

Light-effected kinetic control of host-guest system formation

Having understood the kinetic and thermodynamic behavior of *E*-**2** and α-CD in the absence of light, we studied the interaction between the long-living axle *Z*-**2**, obtained by irradiation at 365 nm (Table S6), and the CD host. First, we performed a ^{1}H NMR titration experiment. The resonance frequency of the axle

Please cite this article in press as: Neira et al., Light-driven ratcheted formation of diastereomeric host-guest systems, Chem (2024), https://doi.org/10.1016/j.chempr.2024.11.013

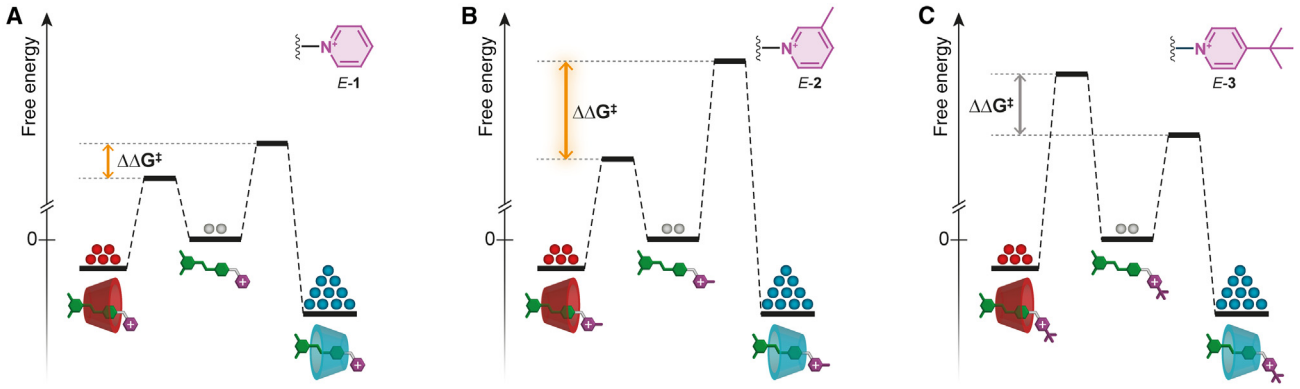

Figure 4. Competitive association of the azobenzene axles with α-CD

Schematic free-energy profiles for the competitive formation of complexes A and B between α-CD and *E*-**1** (A), *E*-**2** (B), and *E*-**3** (C). The distribution of the species is represented by gray, red, and blue spheres corresponding to free axle, complex A, and complex B, respectively.

nuclei underwent minor shifts during the titration, denoting poor interactions between the components (K_Z ~70 M^{-1}; Figure S24).[29] The peaks that were most affected belonged to the aromatic nuclei H_a and H_c, as well as to the methyl protons H_b, all associated with the stopper unit. These observations suggest the minor formation of an *exo*-complex, in which the hydrophobic dimethyl phenyl stopper comes close to the CD cavity. This experiment, in line with literature results,[25–34,49] confirms that the bulky *Z*-azobenzene axle cannot be encapsulated within the α-CD cavity.

The lack of association between *Z*-**2** and α-CD implies that, starting from the *E*-**2** complex, the irradiation with an appropriate wavelength would induce dethreading as a consequence of *E* → *Z* photoisomerization of the complexed *E* axle inside the host cavity. To confirm this, we successfully monitored the photoisomerization of the two types of complexes with a UV-vis spectroscopic technique (Figures S41 and S42; supplemental information section "photokinetic modeling").

To investigate the behavior of the system under illumination, we performed ^{1}H NMR kinetic experiments on a dark-equilibrated solution of axle *E*-**2** and α-CD upon *in situ* irradiation with a UV light-emitting diode (LED) source (369 ± 15 nm) directly connected to a quartz optical fiber (Figure 5A).[50–52]

The dissociation process of the *Z* complex triggered by photoisomerization is too fast to be observed with our techniques. At the PSS obtained upon UV irradiation (369 nm), the solution contained 36% of the *E* complex (18% complex A and 8% complex B) and 74% of the free axle (9% *E*-**2** and 65% *Z*-**2**) (Figure 5B). Remarkably, continuous irradiation favored the formation of the unstable but faster-forming kinetic complex A.

In an analogous experiment, a solution equilibrated in the dark was irradiated with a blue LED source (453 nm) (Figure 5C). Under these conditions, the system reached a PSS in which the kinetic complex A accounted for 45% of the species and was the most abundant moiety. The fraction of free axle was only 37% (17% *E*-**2** and 20% *Z*-**2**) (Figure 5D). These experiments indicate that at 453 nm, the incoming light energy is utilized more efficiently than UV irradiation to accumulate the kinetic product.

DISCUSSION

Operation of the light-driven association

We can interpret the experimental results by analyzing the interplay of the self-assembly and photoisomerization reactions in a network consisting of two interconnected square schemes (Figure 6A). Therefore, the following paragraph will provide a description of the phenomena governing the system, and the comprehensive kinetic modeling is reported in supplemental information section "photokinetic modeling."

From a kinetic perspective, the dethreading of the *Z* complexes can be considered irreversible given that the association between the *Z*-**2** guest and α-CD is negligible, and the dissociation of the photogenerated complex is instantaneous on the experimental timescale. Therefore, the sole photoreaction that can occur for the encapsulated axle is the *E* → *Z* photoisomerization of the *E* complexes. These two consecutive and practically unidirectional reactions impart a net directionality in both square schemes, represented by the circular arrows of Figure 6A.

However, this condition is not sufficient to explain the accumulation of complex A under irradiation. Indeed, the kinetic asymmetry[13,53] in the rates of assembly is key to the selective accumulation of complex A. This asymmetry is responsible for the emergence of two competing specular ratcheting mechanisms (red and blue circular arrows in Figure 6A), one of which is more efficient, ultimately resulting in the driven formation of complex A.

The mechanism can be further explained by the reaction profiles depicted in Figure 6B. In the dark, the system is composed of the free *E*-**2** axle together with complexes A and B, the latter of which is the predominant species at equilibrium (Figure 6B, stage I). Irradiation of the system induces *E* → *Z* photoisomerization, leading to the formation of unstable *Z* complexes that rapidly disassemble into free *Z*-**2** (Figure 6B, stage II). Subsequently, the absorption of further photons triggers the reverse photoisomerization of free *Z*-**2** into *E*-**2**. The photogenerated *E* axle is now more rapidly complexed to yield complex A (Figure 6B, stage III). Under continuous irradiation, the progressive repetition of these steps allows the autonomous light-driven

Please cite this article in press as: Neira et al., Light-driven ratcheted formation of diastereomeric host-guest systems, Chem (2024), https://doi.org/10.1016/j.chempr.2024.11.013

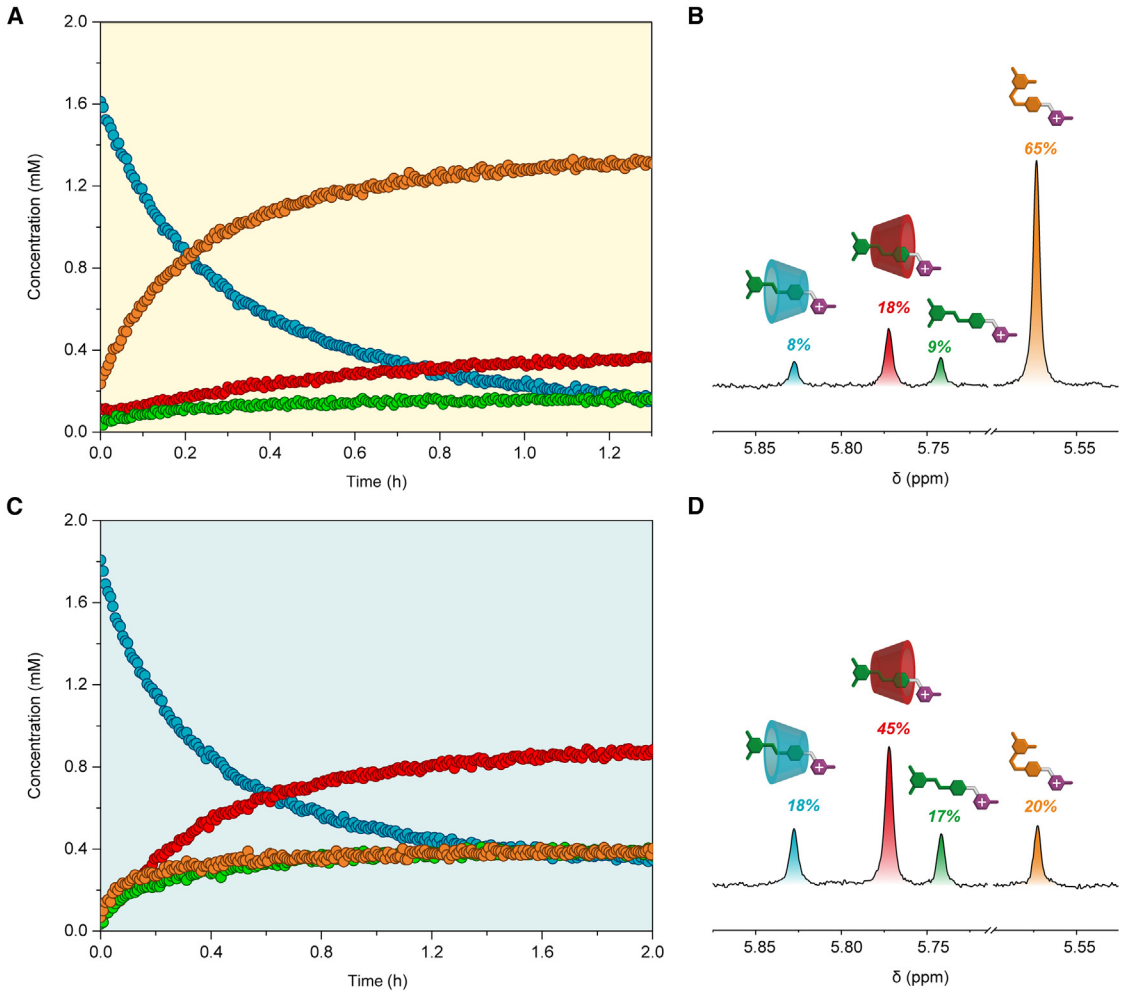

Figure 5. Irradiation experiments of the complexes

(A) ^{1}H NMR concentration profiles (500 MHz, D_2O, 298 K) observed upon irradiation with UV light (369 ± 15 nm) and starting from an equilibrated solution of *E*-**2** (2.0 mM) and α-CD (5.0 mM).

(B) Partial ^{1}H NMR spectrum showing the resonance of H_f in *E*-**2** after exhaustive UV light irradiation.

(C) ^{1}H NMR concentration profiles (500 MHz, D_2O, 298 K) observed upon irradiation with blue light (453 ± 15 nm) and starting from an equilibrated solution of axle *E*-**2** (2.0 mM) and α-CD (5.0 mM).

(D) Partial ^{1}H NMR spectrum showing the resonance of H_f in *E*-**2** after exhaustive blue light irradiation. For both graphs, traces are shown as follows: red, complex A; blue, complex B; green, free axle *E*-**2**; orange, free axle *Z*-**2**.

preferential formation of complex A (Figure 6B, stage IV). In this context, the dependance of the accumulation of complex A on the irradiation wavelength is due to the ratio of *E* and *Z* isomers at the PSSs: UV light produces a higher amount of *Z* isomers, unable to form complexes, whereas visible light leads to a greater proportion of *E* isomers, readily available for complexation. Consequently, visible light proves more effective for accumulating complex A, enhancing the efficiency of the light-driven non-equilibrium distribution.

Considering this ratchet mechanism, the light-driven preferential formation of complex A can be obtained in a shorter timescale than achieved by previous experiments (Figure 5) by operating under different experimental conditions: (1) starting the irradiation immediately after mixing both components when complex A is the predominant species in solution before the thermodynamic equilibration (Figure S53) and (2) in a sequential experiment, inducing the dissociation of the complexes by UV irradiation and subsequently promoting $Z \rightarrow E$ isomerization with visible light to prompt the ratcheted-driven formation of complex A (Figure S54).

Conclusions

We investigated a family of oriented azobenzene-based photoswitchable axles that exhibit high association constants with α-CD in water. Because of the non-symmetric nature of the CD host, two distinct orientational diastereomers are formed upon complexation. By strategically modifying the substituents on the pyridinium terminus of the axles, we were able to fine-tune the kinetic constants associated with the threading and dethreading processes. After a detailed investigation of the complexation

Please cite this article in press as: Neira et al., Light-driven ratcheted formation of diastereomeric host-guest systems, Chem (2024), https://doi.org/10.1016/j.chempr.2024.11.013

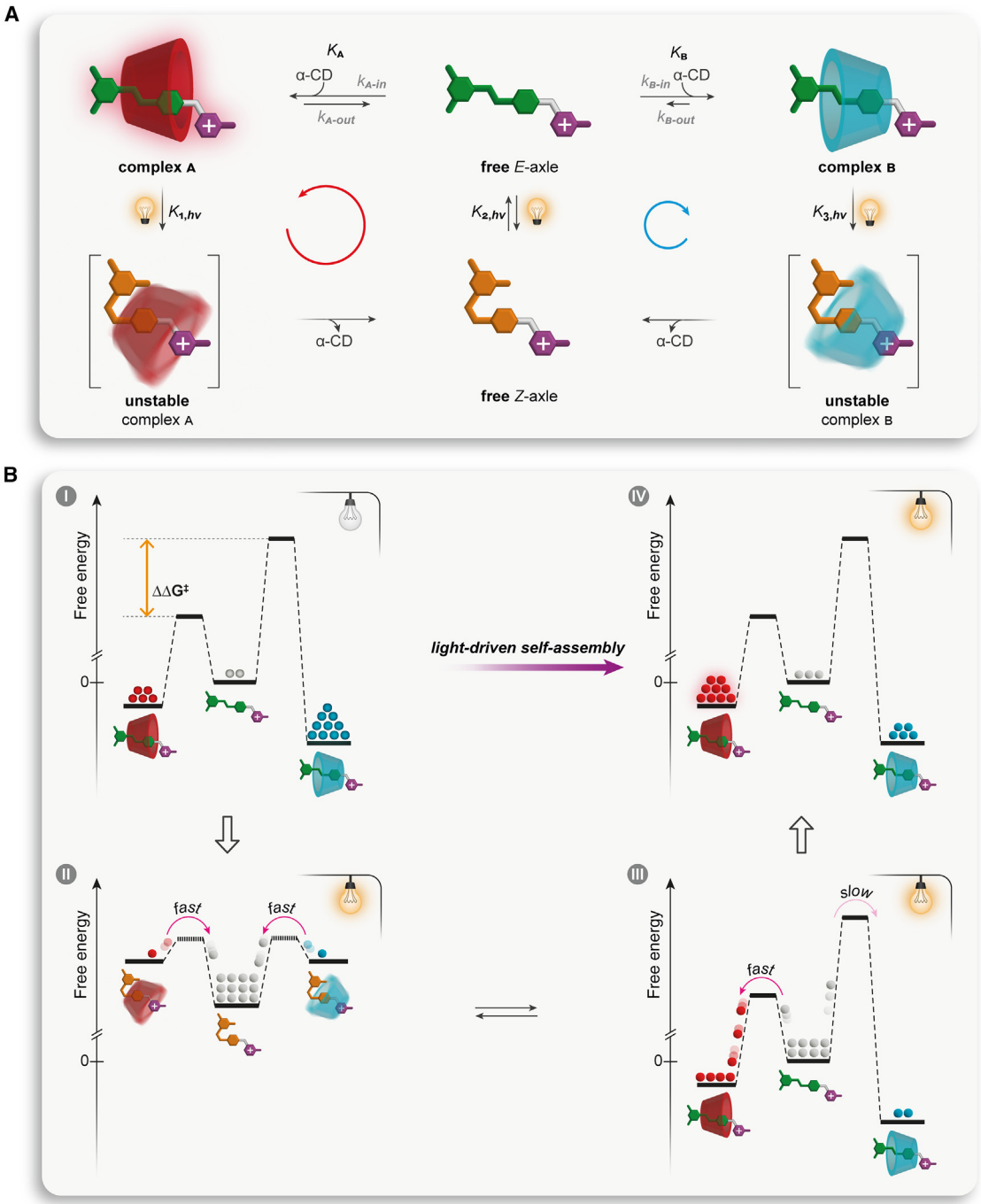

Figure 6. Light-driven formation of complex A

(A) Network of interconnected complexation and $E \rightleftarrows Z$ photoisomerization reactions occurring in a system composed of axles **2** and α-CD.

(B) Schematic free-energy profiles for two competitive equilibria in the dark (I) and under continuous light irradiation (II to IV). The repeated phototriggered switching between profiles II and III leads to non-equilibrium distributions of the products under continuous light irradiation (IV).

reaction of the three axles with α-CD, we focused on guest *E*-**2**, which showed the highest kinetic selectivity for the accumulation of the metastable complex A.

Our study demonstrates that the relative abundance of the two orientational isomers can be shifted from a thermally equilibrated distribution in the dark to a non-equilibrium one under light irradiation, resulting in the population of complex A.

Notably, kinetic control with visible light proved more advantageous than that with UV light given that visible photoirradiation affords a PSS richer in the *E* isomer. This aspect is of great

significance because it allows one to control the diastereoselectivity of the host-guest complex formation by tuning the irradiation wavelength.

The present results extend the vast knowledge on CD host-guest complexes, typically investigated at chemical equilibrium, toward dissipative non-equilibrium regimes sustained by light irradiation. The system represents the first demonstration of a ratcheting synthesis of CD supramolecular complexes in an aqueous environment. Moreover, it contributes to a deeper understanding of the energy uptake and transformation within a system of multiple reactions.

The general validity of the mechanism described and the ample choice of guests for CDs render our findings amenable to development in various contexts. Additionally, the possibility of operating the network in water and using visible light enhances the potential for future applications in diverse fields,[54] including the assembly of life-like systems operating in physiological conditions, the engineering of supramolecular active materials, and the realization of artificial molecular motors that operate in an aqueous environment.

METHODS

Detailed methods can be found in the supplemental information.

RESOURCE AVAILABILITY

Lead contact

Requests for further information and resources should be directed to and will be fulfilled by the lead contact, Prof. Alberto Credi (alberto.credi@unibo.it).

Materials availability

The compounds generated in this study are available from the lead contact upon reasonable request.

Data and code availability

All data needed to support the conclusions of this manuscript are included in the main text or the supplemental information.

ACKNOWLEDGMENTS

Financial support from the European Union – Next Generation EU – and Italian Ministry of University and Research (PRIN grants 2022JMTLE, 201732PY3X, and 2022KMMAYM_002) is gratefully acknowledged. We are thankful for funding received from MCIN/AEI/10.13039/501100011033, the European Regional Development Fund "A way of making Europe" (PID2022-137361NB-I00), and the Consellería de Cultura, Educación e Universidade da Xunta de Galicia (ED431C 2022/39). I.N. gratefully acknowledges NextGenerationEU/PRTR (Margarita Salas program).

AUTHOR CONTRIBUTIONS

Conceptualization, I.N., C.T., F.N., and A.C.; investigation – synthesis, I.N.; investigation – NMR, I.N., F.N., and M.C.; investigation – UV-vis, C.T. and S.S.; formal analysis, I.N., C.T., F.N., M.B., and S.S; writing – original draft, I.N., C.T., and F.N.; writing – review and editing, M.C., M.D.G., C.P., S.S., M.B., and A.C.; visualization, C.T. and C.P.; funding acquisition, M.D.G., C.P., S.S., M.B., and A.C.

DECLARATION OF INTERESTS

The authors declare no competing interests.

SUPPLEMENTAL INFORMATION

Supplemental information can be found online at https://doi.org/10.1016/j.chempr.2024.11.013.

Received: June 24, 2024
Revised: July 22, 2024
Accepted: November 20, 2024
Published: December 27, 2024

REFERENCES

1. Crini, G. (2014). Review: a history of cyclodextrins. Chem. Rev. *114*, 10940–10975. https://doi.org/10.1021/cr500081p.
2. Rekharsky, M.V., and Inoue, Y. (1998). Complexation thermodynamics of cyclodextrins. Chem. Rev. *98*, 1875–1918. https://doi.org/10.1021/cr970015o.
3. Blanco-Gómez, A., Cortón, P., Barravecchia, L., Neira, I., Pazos, E., Peinador, C., and García, M.D. (2020). Controlled binding of organic guests by stimuli-responsive macrocycles. Chem. Soc. Rev. *49*, 3834–3862. https://doi.org/10.1039/d0cs00109k.
4. Bruns, C.J. (2019). Exploring and exploiting the symmetry-breaking effect of cyclodextrins in mechanomolecules. Symmetry *11*, 1249–1271. https://doi.org/10.3390/sym11101249.
5. Wu, Y., Aslani, S., Han, H., Tang, C., Wu, G., Li, X., Wu, H., Stern, C.L., Guo, Q.-H., Qiu, Y., et al. (2024). Mirror-image cyclodextrins. Nat. Synth. *3*, 698–706. https://doi.org/10.1038/s44160-024-00495-8.
6. Oshikiri, T., Takashima, Y., Yamaguchi, H., and Harada, A. (2005). Kinetic control of threading of cyclodextrins onto axle molecules. J. Am. Chem. Soc. *127*, 12186–12187. https://doi.org/10.1021/ja053532u.
7. Oshikiri, T., Takashima, Y., Yamaguchi, H., and Harada, A. (2007). Face-selective [2]- and [3]rotaxanes: kinetic control of the threading direction of cyclodextrins. Chemistry *13*, 7091–7098. https://doi.org/10.1002/chem.200601657.
8. Hashidzume, A., Kuse, A., Oshikiri, T., Adachi, S., Okumura, M., Yamaguchi, H., and Harada, A. (2018). Toward a translational molecular ratchet: face-selective translation coincident with deuteration in a pseudo-rotaxane. Sci. Rep. *8*, 8950. https://doi.org/10.1038/s41598-018-27226-2.
9. Seeman, J.I. (1986). The Curtin-Hammett principle and the Winstein-Holness equation: new definition and recent extensions to classical concepts. J. Chem. Educ. *63*, 42–48. https://doi.org/10.1021/ed063p42.
10. Seeman, J.I. (1983). Effect of conformational change on reactivity in organic chemistry. Evaluations, applications, and extensions of Curtin-Hammett Winstein-Holness kinetics. Chem. Rev. *83*, 83–134. https://doi.org/10.1021/cr00054a001.
11. Andraos, J. (2003). Quantification and optimization of dynamic kinetic resolution. J. Phys. Chem. A *107*, 2374–2387. https://doi.org/10.1021/jp0272365.
12. Anslyn, V., and Dougherty, D.A. (2006). Modern Physical Organic Chemistry (University Science Books).
13. Amano, S., Esposito, M., Kreidt, E., Leigh, D.A., Penocchio, E., and Roberts, B.M.W. (2022). Using catalysis to drive chemistry away from equilibrium: relating kinetic asymmetry, power strokes, and the Curtin-Hammett principle in Brownian ratchets. J. Am. Chem. Soc. *144*, 20153–20164. https://doi.org/10.1021/jacs.2c08723.
14. Takahashi, S., Sato, H., and Hiraoka, S. (2023). Extended Curtin-Hammett principle: origin of pathway selection in reversible reaction networks under kinetic control. Preprint at ChemRxiv. https://doi.org/10.26434/chemrxiv-2023-37qp8.
15. Mattia, E., and Otto, S. (2015). Supramolecular systems chemistry. Nat. Nanotechnol. *10*, 111–119. https://doi.org/10.1038/nnano.2014.337.
16. Sorrenti, A., Leira-Iglesias, J., Markvoort, A.J., De Greef, T.F.A., and Hermans, T.M. (2017). Non-equilibrium supramolecular polymerization. Chem. Soc. Rev. *46*, 5476–5490. https://doi.org/10.1039/C7CS00121E.

17. Zhang, Y., Xu, Z., Jiang, T., Fu, Y., and Ma, X. (2023). A time-resolved and visualized host–guest self-assembly behavior controlled through kinetic trapping. J. Mater. Chem. C *11*, 1742–1746. https://doi.org/10.1039/D2TC05112E.

18. Li, G., Lewis, R.W., and Eelkema, R. (2024). Out-of-equilibrium assembly based on host–guest interactions. CCS Chem. *6*, 27–40. https://doi.org/10.31635/ccschem.023.202303177.

19. Sangchai, T., Al Shehimy, S., Penocchio, E., and Ragazzon, G. (2023). Artificial molecular ratchets: tools enabling endergonic processes. Angew. Chem. Int. Ed. *62*, e202309501. https://doi.org/10.1002/anie.202309501.

20. Kathan, M., Eisenreich, F., Jurissek, C., Dallmann, A., Gurke, J., and Hecht, S. (2018). Light-driven molecular trap enables bidirectional manipulation of dynamic covalent systems. Nat. Chem. *10*, 1031–1036. https://doi.org/10.1038/s41557-018-0106-8.

21. Borsley, S., Gallagher, J.M., Leigh, D.A., and Roberts, B.M.W. (2024). Ratcheting synthesis. Nat. Rev. Chem. *8*, 8–29. https://doi.org/10.1038/s41570-023-00558-y.

22. Ragazzon, G., and Prins, L.J. (2018). Energy consumption in chemical fuel-driven self-assembly. Nat. Nanotechnol. *13*, 882–889. https://doi.org/10.1038/s41565-018-0250-8.

23. Das, K., Gabrielli, L., and Prins, L.J. (2021). Chemically fueled self-assembly in biology and chemistry. Angew. Chem. Int. Ed. *60*, 20120–20143. https://doi.org/10.1002/anie.202100274.

24. Harada, A. (2001). Cyclodextrin-based molecular machines. Acc. Chem. Res. *34*, 456–464. https://doi.org/10.1021/ar000174l.

25. Inoue, Y., Kuad, P., Okumura, Y., Takashima, Y., Yamaguchi, H., and Harada, A. (2007). Thermal and photochemical switching of conformation of poly(ethylene glycol)-substituted cyclodextrin with an azobenzene group at the chain end. J. Am. Chem. Soc. *129*, 6396–6397. https://doi.org/10.1021/ja071717q.

26. Lerch, M.M., Hansen, M.J., Velema, W.A., Szymanski, W., and Feringa, B.L. (2016). Orthogonal photoswitching in a multifunctional molecular system. Nat. Commun. *7*, 12054. https://doi.org/10.1038/ncomms12054.

27. Tarn, D., Ferris, D.P., Barnes, J.C., Ambrogio, M.W., Stoddart, J.F., and Zink, J.I. (2014). A reversible light-operated nanovalve on mesoporous silica nanoparticles. Nanoscale *6*, 3335–3343. https://doi.org/10.1039/C3NR06049G.

28. Ferris, D.P., Zhao, Y.-L., Khashab, N.M., Khatib, H.A., Stoddart, J.F., and Zink, J.I. (2009). Light-operated mechanized nanoparticles. J. Am. Chem. Soc. *131*, 1686–1688. https://doi.org/10.1021/ja807798g.

29. Liao, X., Chen, G., Liu, X., Chen, W., Chen, F., and Jiang, M. (2010). Photoresponsive pseudopolyrotaxane hydrogels based on competition of host-guest interactions. Angew. Chem. Int. Ed. *49*, 4409–4413. https://doi.org/10.1002/anie.201000141.

30. Höglsperger, F., Larik, F.A., Bai, C., Seyfried, M.D., Daniliuc, C., Klaasen, H., Thordarson, P., Beves, J.E., and Ravoo, B.J. (2023). Water-soluble arylazoisoxazole photoswitches. Chemistry *29*, e202302069. https://doi.org/10.1002/chem.202302069.

31. Quan, J., Guo, Y., Ma, J., Long, D., Wang, J., Zhang, L., Sun, Y., Dhinakaran, M.K., and Li, H. (2022). Light-responsive nanochannels based on the supramolecular host–guest system. Front. Chem. *10*, 986908. https://doi.org/10.3389/fchem.2022.986908.

32. Wan, P., Jiang, Y., Wang, Y., Wang, Z., and Zhang, X. (2008). Tuning surface wettability through photocontrolled reversible molecular shuttle. Chem. Commun. *2008*, 5710–5712. https://doi.org/10.1039/B811729B.

33. Wang, J., Zhang, Y.-M., Zhang, X.-J., Zhao, X.-J., and Liu, Y. (2015). Light-controlled [3]pseudorotaxane based on tetrasulfonated 1,5-dinaphtho-32-crown-8 and α-cyclodextrin. Asian J. Org. Chem. *4*, 244–250. https://doi.org/10.1002/ajoc.201402238.

34. Iwaso, K., Takashima, Y., and Harada, A. (2016). Fast response dry-type artificial molecular muscles with [c2]daisy chains. Nat. Chem. *8*, 625–632. https://doi.org/10.1038/nchem.2513.

35. Ragazzon, G., Baroncini, M., Silvi, S., Venturi, M., and Credi, A. (2015). Light-powered autonomous and directional molecular motion of a dissipative self-assembling system. Nat. Nanotechnol. *10*, 70–75. https://doi.org/10.1038/nnano.2014.260.

36. Nicoli, F., Curcio, M., Tranfić Bakić, M., Paltrinieri, E., Silvi, S., Baroncini, M., and Credi, A. (2022). Photoinduced autonomous nonequilibrium operation of a molecular shuttle by combined isomerization and proton transfer through a catalytic pathway. J. Am. Chem. Soc. *144*, 10180–10185. https://doi.org/10.1021/jacs.1c13537.

37. Gemen, J., Church, J.R., Ruoko, T.P., Durandin, N., Białek, M.J., Weißenfels, M., Feller, M., Kazes, M., Odaybat, M., Borin, V.A., et al. (2023). Disequilibrating azobenzenes by visible-light sensitization under confinement. Science *381*, 1357–1363. https://doi.org/10.1126/science.adh9059.

38. DiNardi, R.G., Douglas, A.O., Tian, R., Price, J.R., Tajik, M., Donald, W.A., and Beves, J.E. (2022). Visible-light-responsive self-assembled complexes: improved photoswitching properties by metal ion coordination. Angew. Chem. Int. Ed. *61*, e202205701. https://doi.org/10.1002/anie.202205701.

39. Kathan, M., and Hecht, S. (2017). Photoswitchable molecules as key ingredients to drive systems away from the global thermodynamic minimum. Chem. Soc. Rev. *46*, 5536–5550. https://doi.org/10.1039/C7CS00112F.

40. Ovalle, M., Kathan, M., Toyoda, R., Stindt, C.N., Crespi, S., and Feringa, B.L. (2023). Light-fueled transformations of a dynamic cage-based molecular system. Angew. Chem. Int. Ed. *62*, e202214495. https://doi.org/10.1002/anie.202214495.

41. Yin, Z., Song, G., Jiao, Y., Zheng, P., Xu, J.-F., and Zhang, X. (2019). Dissipative supramolecular polymerization powered by light. CCS Chem. *1*, 335–342. https://doi.org/10.31635/ccschem.019.20190013.

42. Hou, X.-F., Chen, X.-M., Bisoyi, H.K., Qi, Q., Xu, T., Chen, D., and Li, Q. (2023). Light-driven aqueous dissipative pseudorotaxanes with tunable fluorescence enabling deformable nano-assemblies. ACS Appl. Mater. Interfaces *15*, 11004–11015. https://doi.org/10.1021/acsami.2c20276.

43. Herder, M., and Lehn, J.-M. (2018). The photodynamic covalent bond: sensitized alkoxyamines as a tool to shift reaction networks out-of-equilibrium using light energy. J. Am. Chem. Soc. *140*, 7647–7657. https://doi.org/10.1021/jacs.8b03633.

44. Baglai, I., Leeman, M., Kaptein, B., Kellogg, R.M., and Noorduin, W.L. (2019). A chiral switch: balancing between equilibrium and non-equilibrium states. Chem. Commun. *55*, 6910–6913. https://doi.org/10.1039/C9CC03250A.

45. Liu, E., Cherraben, S., Boulo, L., Troufflard, C., Hasenknopf, B., Vives, G., and Sollogoub, M. (2023). A molecular information ratchet using a cone-shaped macrocycle. Chem *9*, 1147–1163. https://doi.org/10.1016/j.chempr.2022.12.017.

46. Baer, A.J., and Macartney, D.H. (2005). Orientational isomers of α-cyclodextrin [2]semi-rotaxanes with asymmetric dicationic threads. Org. Biomol. Chem. *3*, 1448–1452. https://doi.org/10.1039/B418055K.

47. Merino, E. (2011). Synthesis of azobenzenes: the coloured pieces of molecular materials. Chem. Soc. Rev. *40*, 3835–3853. https://doi.org/10.1039/C0CS00183J.

48. Schönbeck, C. (2018). Charge determines guest orientation: a combined NMR and molecular dynamics study of β-cyclodextrins and adamantane derivatives. J. Phys. Chem. B *122*, 4821–4827. https://doi.org/10.1021/acs.jpcb.8b02579.

49. Royes, J., Courtine, C., Lorenzo, C., Lauth-de Viguerie, N., Mingotaud, A.F., and Pimienta, V. (2020). Quantitative kinetic modeling in photoresponsive supramolecular chemistry: the case of water-soluble azobenzene/cyclodextrin complexes. J. Org. Chem. *85*, 6509–6518. https://doi.org/10.1021/acs.joc.0c00461.

50. Corra, S., Bakić, M.T., Groppi, J., Baroncini, M., Silvi, S., Penocchio, E., Esposito, M., and Credi, A. (2022). Kinetic and energetic insights into the

dissipative non-equilibrium operation of an autonomous light-powered supramolecular pump. Nat. Nanotechnol. *17*, 746–751. https://doi.org/10.1038/s41565-022-01151-y.

51. Nitschke, P., Lokesh, N., and Gschwind, R.M. (2019). Combination of illumination and high resolution NMR spectroscopy: key features and practical aspects, photochemical applications, and new concepts. Prog. Nucl. Magn. Reson. Spectrosc. *114–115*, 86–134. https://doi.org/10.1016/j.pnmrs.2019.06.001.

52. Feldmeier, C., Bartling, H., Riedle, E., and Gschwind, R.M. (2013). LED based NMR illumination device for mechanistic studies on photochemical reactions - versatile and simple, yet surprisingly powerful. J. Magn. Reson. *232*, 39–44. https://doi.org/10.1016/j.jmr.2013.04.011.

53. Astumian, R.D. (2024). Kinetic asymmetry and directionality of nonequilibrium molecular systems. Angew. Chem. Int. Ed. *63*, e202306569. https://doi.org/10.1002/anie.202306569.

54. Zhang, Z.Y., Dong, D., Bösking, T., Dang, T., Liu, C., Sun, W., Xie, M., Hecht, S., and Li, T. (2024). Solar azo-switches for effective E→Z photoisomerization by sunlight. Angew. Chem. Int. Ed. *63*, e202404528. https://doi.org/10.1002/anie.202404528.